ARTICLE NO. 79-0095R

Prediction of Rocket Plume Flowfields for Infrared Signature Studies

S.M. Dash,* B.E. Pearce,* H.S. Pergament,† and E.S. Fishburne‡
Aeronautical Research Associates of Princeton, Inc., Princeton, N.J.

The contribution of various gasdynamic processes affecting rocket exhaust plume structure in the altitude range of 0-60 km is discussed in terms of their relative influence on plume infrared radiation signature predictions. It is demonstrated that spatial details of the nearfield inviscid/shock structure in rocket plumes can appreciably affect flight signature levels at higher altitudes (i.e., $h>$ 30-40 km). Spatial details are also required in the analysis of most laboratory plumes. Simplified gasdynamic models which globally incorporate the effects of inviscid structure into the startline conditions for a pressure-equilibrated farfield mixing analysis are shown to be adequate in flight signature studies at lower altitudes (i.e., $h>$ 20-30 km). The sensitivities of rocket plume emission to variations in turbulence modeling parameters are presented for flight signature studies at representative lower and higher altitudes in the range of interest. It is demonstrated that, under all conditions, turbulent mixing processes play a dominant role in the prediction of plume signature levels.

Introduction

THE prediction of exhaust plume radiation involves the application of both gasdynamic and radiative transfer models. Gasdynamic models predict the spatial distribution of temperature and species concentrations within the plume while radiative models predict the infrared radiation emitted and transferred through the plume and intervening atmosphere to a distant sensor. The modeling of radiative transfer within the plume appears to be well in hand in comparison with that of gasdynamic processes. Radiative predictions based on flowfield patterns generated by different gasdynamic models have been found to differ widely. These differences are due primarily to the manner in which the various gasdynamic models analyze nearfield inviscid/shock processes and mixing/afterburning processes in both the near and farfields.

A recent review of plume modeling procedures[1] has shown that the relative contribution of the inviscid/shock and mixing/afterburning processes (and their coupling) is dependent upon vehicle/engine characteristics, flight conditions, the characteristics of the radiation (i.e., opacity and spectral bandpass), and the spatial resolution of the observation. The results presented in Ref. 1 suggest that the details of the inviscid/shock structure should provide a negligible contribution to integrated plume signatures at lower altitudes, and play an increasingly important role at higher altitudes. However, this has not been quantitatively demonstrated. It is the purpose of this paper therefore to: 1) introduce computational procedures which can be used to asses the specific contributions of inviscid/shock and mixing/afterburning processes on plume radiation; and 2) provide such an assessment via a systematic series of calculations for a large liquid propellant booster at representative lower and higher altitudes in the 0-60 km range.

In the next section of this paper, the various gasdynamic processes occurring in rocket plumes are briefly reviewed and modeling techniques for their analysis are described. The subsequent section discusses simplified modeling procedures for including the effects of inviscid/shock structure in the overall analysis. In one approach, the plume is analyzed in a constant pressure mode of operation, and total pressure losses due to shock processes are globally considered in specifying startline conditions for the mixing/afterburning analysis. In the other more detailed approach, the mixing layer is "overlaid" on the independently calculated inviscid pattern. Finally, the sensitivity of rocket plume emission to variations in turbulence parameters is discussed.

Gasdynamic Processes and Modeling Techniques

Overall Plume Structure

In the nearfield of an underexpanded rocket plume (Fig. 1), the exhaust gas equilibrates to ambient pressure levels through a series of shock and expansion waves. Inviscid processes determine the nearfield plume geometry and control the spatial equilibration to ambient pressure levels. At the nozzle lip, an interaction process yields a pressure balance between the underexpanded exhaust gas and the external flow. The ensuing plume interface has a monotonically decreasing slope and generates downward-running compressions into the exhaust flow. These waves coalesce and form a barrel shock which progressively increases in strength, ultimately collapsing to form a Mach disk. The barrel shock divides the exhaust gas into two zones: a core which behaves independently of the external stream, and a barrel shock layer which contains the exhaust gas which has interacted with the external stream. Downstream of the Mach disk location, a reflected shock again divides the exhaust gas into two zones. In addition, a third zone exists, comprising that portion of the exhaust flow which has traversed through the Mach disk. The inviscid cell terminates at the axial station at which the reflected shock intersects the plume interface. The same type of pattern occurs in subsequent inviscid cells subject to an overall decay by diffusive processes.

In the nearfield, turbulent mixing processes are confined to the thin shear layers growing along the plume interface and the Mach disk slipstream. Afterburning of excess fuel or

Presented as Paper 79-0095 at the 17th Aerospace Sciences Meeting, New Orleans, La., Jan. 15-17, 1979; submitted Feb. 14, 1979; revision received Oct. 15, 1979.

Index categories: Jets, Wakes, and Viscous/Inviscid Flow Interactions; Radiation and Radiative Heat Transfer; Computational Methods.

*Consultants, Aerophysics Department. Members AIAA.
†Senior Consultant, Head of Aerophysics Department.
‡Currently President, Scientific Technology Associates, Inc. Member AIAA.

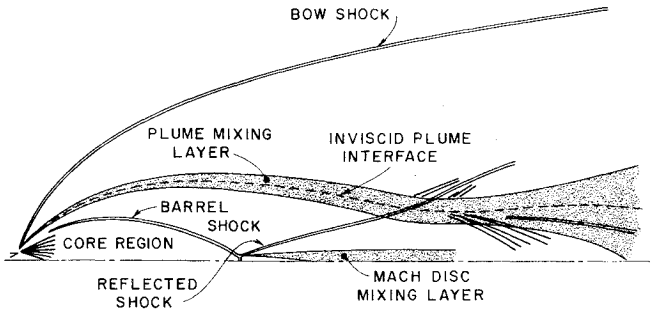

Fig. 1 Schematic of viscous/inviscid structure in plume nearfield.

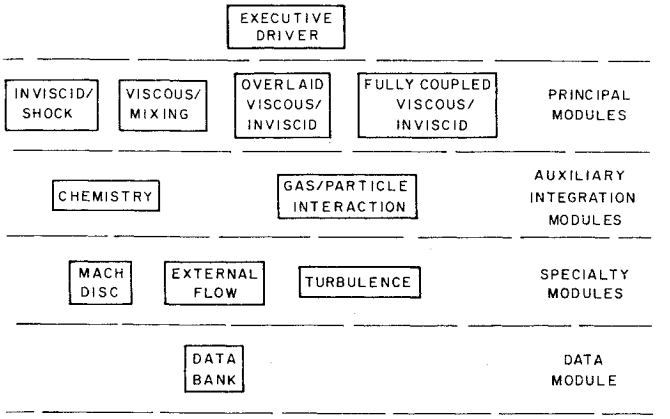

Fig. 2 Modular structure in new standard plume flowfield model.

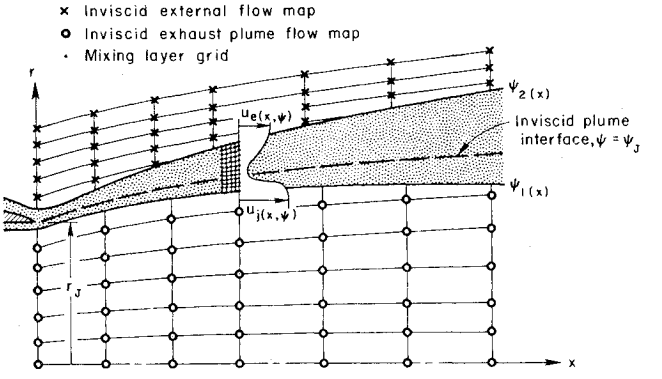

Fig. 3 Shear layer overlaid on inviscid flow pattern.

intermediate exhaust products with entrained air can be initiated in the plume shear layer. Finite-rate chemical processes also are important in establishing the temperature and composition of the flow within the Mach disk stream tube.

In the farfield, turbulent mixing and afterburning processes continue under essentially constant pressure conditions. Here, the variations in local temperatures and pressures associated with the inviscid structure have been largely damped through the dissipative losses associated with shock waves and turbulent mixing. In contrast to the nearfield, farfield processes are relatively straightforward to analyze. Constant pressure mixing processes are governed by a parabolic system of partial differential equations which are solved by finite-difference procedures, and the coupling of finite-rate chemical processes into this system is routine. The uncertainties in the farfield analysis reside in the turbulence modeling parameters and rate constants for the chemical system of interest, as well as upon the initial conditions of mean flow and turbulence properties which are determined by the nearfield analysis.

Gasdynamic Modeling Techniques

To date, the Low Altitude Plume Program (LAPP)[2] has been the most widely used flowfield model for signature applications. LAPP analyzes turbulent mixing and afterburning processes in exhaust plumes at constant pressure and does not account for the *spatial* expansion to ambient pressure occurring in the nearfield. In early applications of LAPP, the underexpanded exhaust gas mixture was isentropically expanded to ambient pressure, yielding startline conditions for the constant pressure mixing/afterburning analysis. More recently, the "global" effects of exhaust shock structure have been considered by including the total pressure losses in the expansion processes. This improvement yields higher startline temperatures, lower velocities, and larger radii than the isentropic expansion.

Since LAPP's inception, substantial progress has been made in developing computational methods for analyzing rocket plume exhaust flowfields (see Ref. 1). This methodology includes procedures for the coupling of viscous and inviscid processes in interactive or noninteractive modes providing a detailed portrayal of the complex plume structure in the nearfield. A new standardized plume flowfield model[3,4] (SPF) is presently under development whose objective is to consolidate the "best" of such methodology into a user-oriented computer code. In view of the many processes entering into a detailed plume calculation, a modular approach had been selected as schematized in Fig. 2. This approach permits adjusting the overall mode of operation to match the requirements imposed by the case under consideration. This paper will serve to establish guidelines stipulating operating modes for the SPF in application to flight signature studies.

The analysis of mixing and afterburning processes in the new SPF will be based on the procedures incorporated in the BOAT code.[5,6] BOAT is the successor to LAPP, retaining the same efficient streamline integration techniques and implicit treatment of generalized chemical systems while providing significant improvements over LAPP with respect to: computational domain and grid distribution, solution of the energy equation, boundary growth formulation, inclusion of two-equation turbulence models, and generalized initialization procedures. BOAT has been used to assess several turbulence models for plume applications via comparisons of predictions with a large body of fundamental laboratory data as detailed in Refs. 7 and 8.

A highly distinctive capability of BOAT resides in its ability to analyze thin nearfield shear layers with variable pressure gradients and edge conditions. This is accomplished via an "overlaid" procedure (Fig. 3). Here, the inviscid structure is determined a priori, in the absence of any viscous influence. Viscous processes in the thin shear layers are then analyzed via a boundary layer type of approximation, with the pressure gradients and edge conditions set in accordance with the inviscid pattern. This "overlaid" approach was first introduced in the GASL Rocket Plume Model[9] and has been validated by comparisons with nearfield experimental measurements for several laboratory rocket plumes.[1] An interactive extension of this overlaid procedure has been developed for analyzing the nearfield region of aircraft plumes with large external boundary layers, whose details and validation are available in Refs. 5,6, and 10.

Inviscid processes in the SPF will be based on the procedures incorporated in the SCIPPY code.[11] SCIPPY integrates the supersonic flowfield equations employing one-sided finite-difference procedures at interior points and characteristic procedures at boundaries. Shock processes are analyzed by both capturing and fitting procedures. A generalized class of supersonic flowfield problems can be analyzed via the use of a multiple mapped domain approach implemented with respect to three (cartesian, cylindrical, and spherical) coordinate systems. Domain boundaries include centerlines and symmetry planes, interfaces, shock and

characteristic surfaces, and solid surfaces. Predictions employing SCIPPY have been reported in Refs. 3, 4, and 12.

The coupling of viscous and inviscid flow processes in a noninteractive overlaid fashion provides a simple method for analyzing the nearfield region of the plume. In past applications of the overlaid procedure, it was shown that the predominant shock heating (entropy production) occurs in the first inviscid cell.[1] In addition, the pressure levels achieved at the end of the first inviscid cell are relatively close to ambient. For higher altitude plumes, rather marked excursions in pressure occur in the first inviscid cell, while the pressure excursions in the second and subsequent cells tend to be relatively small. This is illustrated in Fig. 4 which depicts the calculated centerline pressure variation in the first two inviscid cells of a higher altitude rocket exhaust plume. These observations imply that calculating a single inviscid cell might be all that is necessary in representing that inviscid structure for signature studies.

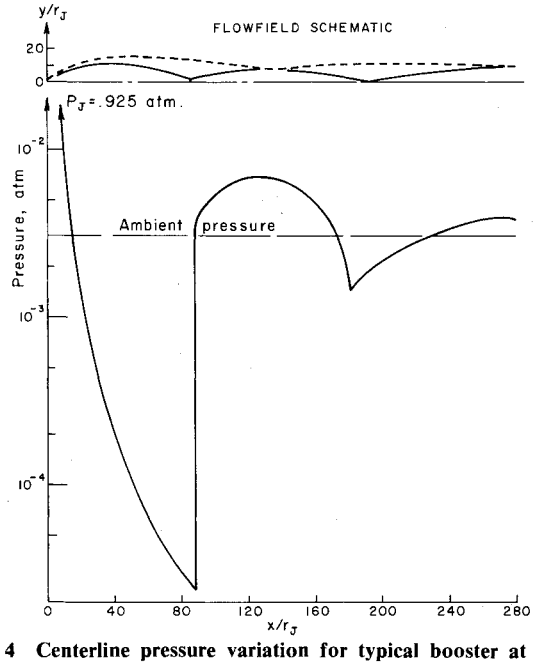

Fig. 4 Centerline pressure variation for typical booster at higher altitude.

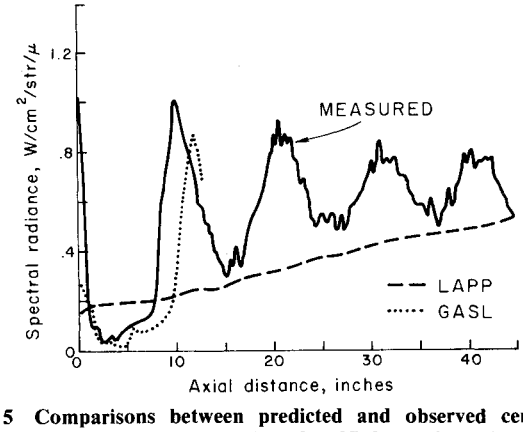

Fig. 5 Comparisons between predicted and observed centerline radiometric data: nozzle lip half angle = 27 deg, exit static pressure ratio = 4.5 (from Ref. 1).

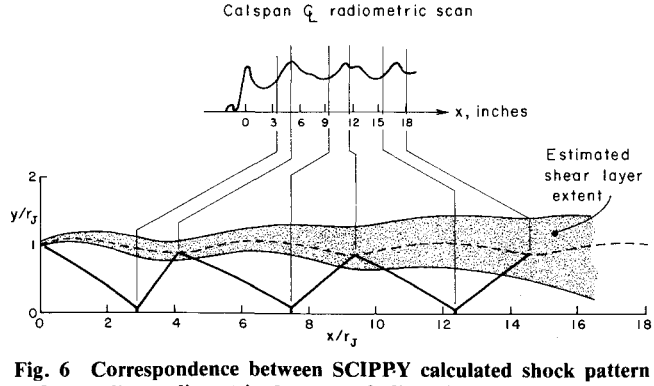

Fig. 6 Correspondence between SCIPPY calculated shock pattern and centerline radiometric data: nozzle lip half angle = 10 deg, exit static pressure ratio ~ 1.

In the analysis of laboratory plumes, the details of the inviscid spatial structure can strongly affect the local plume emission. These details may persist for several inviscid cells as exhibited in Fig. 5. Clearly, constant pressure mixing models, such as LAPP,[2] cannot account for the local shock induced excursions in radiance. Overlaid models can be expected to do a reasonable job in the span of the first inviscid cell (within the framework of uncertainties in the intitial conditions, turbulence parameters, and chemical production rates). Beyond the first inviscid cell, the plume shear layer thickness can be rather substantial and interactive effects associated with the coupling of viscous and inviscid processes can then become significant. The direct correspondence between inviscid structure (as calculated by the SCIPPY code) and centerline radiometric data is illustrated in Fig. 6. That data displays a decay in intensity from exit plane to Mach disk locations and a rise to maximum intensity at the end of the inviscid cells. The smaller lip angle and pressure mismatch in this case lead to relatively small excursions in radiance and a slower cell-to-cell decay in comparison with the case illustrated in Fig. 5. It should be noted that the inviscidly predicted wave locations do not accurately match the data beyond the second inviscid cell due to the neglect of viscous/inviscid interactions.

In the SPF, an integration module will be available which provides for the detailed analysis of the fully coupled viscous-inviscid equations. Preliminary results obtained employing this module have been reported in Refs. 4 and 13. This module can be applied to the analysis of laboratory plumes where interactive effects can be important in interpreting the highly spatially resolved IR measurements. Interactive effects also can be appreciable in the nearfield shear layer when adjacent to a base or separated region and at higher altitudes where large vortical layers occur. Such vortical layers occur: 1) in the external stream along the plume interface (i.e., in the entropy layer comprised of that portion of the airstream that has crossed the nose region of the detached bow shock); and 2) along the Mach disk slipstream (comprised of that portion of the exhaust flow which has traversed the combined barrel/reflected shock system in the vicinity of the axis, where the nonlinear shock strengthening produces an equivalent entropy layer effect).

Radiative Transfer Model

The AARAD code[14] was employed for the radiative calculations reported herein. AARAD utilizes a band model formulation for the prediction of emission from non-homogeneous, axisymmetric plumes and can account for arbitrary aspect angle of observation, obscuration by intervening opaque surfaces, and transmission through the plume of emission from hot opaque surfaces. Only broadside observational conditions with no obscuration are reported herein.

Band model parameters are updated values[15,16] given in frequency intervals of 25 cm^{-1} or less. Spectral intensities presented here were computed for spectral intervals of 5-10 cm^{-1}. The spatial resolution through the plume can be specified arbitrarily, the only limitation being computational time. All intensities presented are for the source alone, without atmospheric attenuation.

Contribution of Inviscid/Shock Processes in Full-Scale Signature Studies

Pressure-Equilibrated Approach

A simple and widely used approach in signature-oriented studies involves the complete neglect of the nearfield inviscid spatial structure. The underexpanded exhaust is abruptly expanded to ambient pressure yielding startline conditions for a subsequent constant pressure mixing/afterburning analysis. To account for the "global" effects of exhaust shock structure, the averaged total pressure losses are incorporated into the startline expansion. The direct relationship between plume drag and averaged total pressure losses permits the use of simplified relations in their estimation. A recent simplified approach for estimating these total pressure losses had been given by Sukanek.[17] Comparisons with results obtained using the SCIPPY code[11] indicated that the total pressure losses predicted by the Sukanek method were excessive. This was found to be caused by an inconsistent specification of the plume drag.[18] The "corrected" analysis[18] now yields startline conditions that agree quite well with those based on the results of SCIPPY and another inviscid computational model.[19] Average startline temperatures for a typical liquid booster are depicted in Fig. 7 for: an isentropic expansion, the "corrected" Sukanek method,[18] the original Sukanek method,[17] and detailed numerical models.

The temperature boosts associated with the shock (total pressure) losses are seen to be quite substantial at the higher altitudes. To portray the nonlinear altitude dependency more clearly, the "corrected" startline values of temperature, velocity, and plume radius are shown normalized by the corresponding isentropic startline values in Fig. 8. At altitudes below 20 km temperature boosts are less than about 5%, while above 40 km they are greater than about 15%. The specific contribution of these boosts alone is expected to be rather small at altitudes below 20 km (i.e., at 20 km, the temperature difference is about 50 K against an average plume temperature of about 1100 K) and rather substantial at altitudes above 40 km (i.e., the temperature difference here is over 100 K against an average plume temperature of about 700 K).

Limitations of Pressure-Equilibrated Approach

Having established that simplified procedures can indeed predict reasonable estimates for the plume drag and, hence, averaged startline conditions, an issue of even greater importance arises—viz, the overall adequacy of neglecting the spatial effects of inviscid structure. The pressure-equilibrated approach, while "globally" accounting for shock losses does not account for nearfield variations of pressure and temperature due to wave processes or nonuniformities in startline conditions for the farfield mixing due to variable shock strengths.

Temperature profiles at several stations in the nearfield of the aforementioned booster at the higher altitude (Fig. 9) depict the large variations associated with the shock and expansion waves. Nonuniform pressure-equilibrated startline temperatures for this booster at representative lower and higher altitudes (Fig. 10) depict the variations associated with nonlinear shock strengthening near the axis and are compared with uniform isentropic and nonisentropic startline values.

The inviscidly induced nearfield variations can produce excursions in the local station radiation which, in certain situations, can affect the overall signature level. These variations also can indirectly affect plume emissions through their influence on mixing and afterburning processes in the nearfield. It is well known that the rates of turbulent mixing are directly related to the shear layer edge conditions, which substantially vary in the plume nearfield. In addition, turbulent mixing rates have been shown to be enhanced in regions of adverse pressure gradients and diminished in regions of favorable pressure gradients.[20] The dependence of

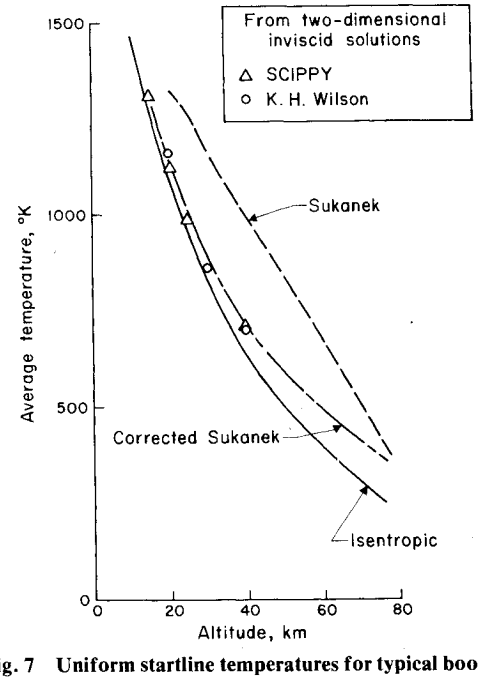

Fig. 7 Uniform startline temperatures for typical booster.

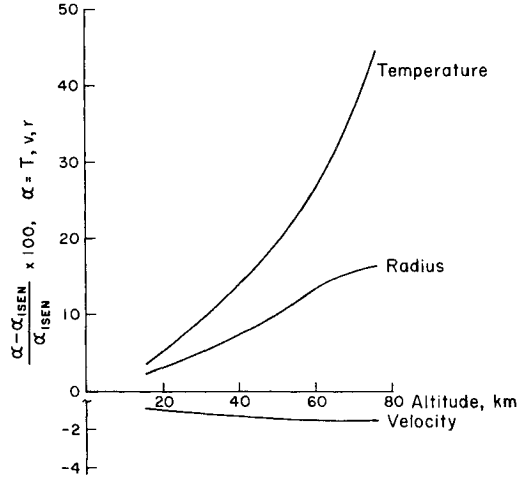

Fig. 8 Percentage increments in noninsentropic startline properties with respect to isentropic values.

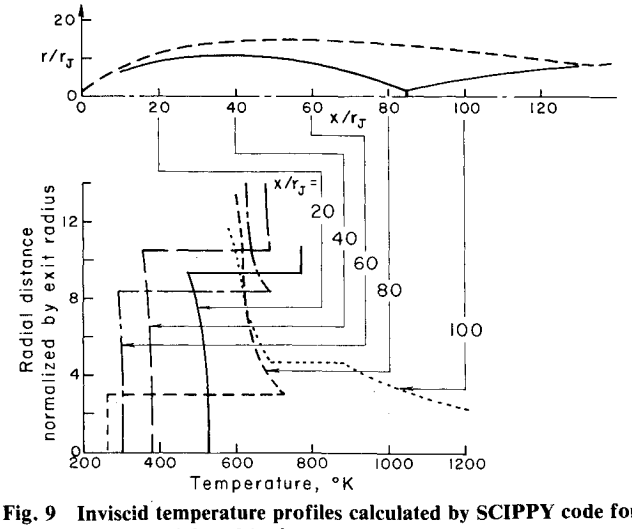

Fig. 9 Inviscid temperature profiles calculated by SCIPPY code for typical booster at higher altitude.

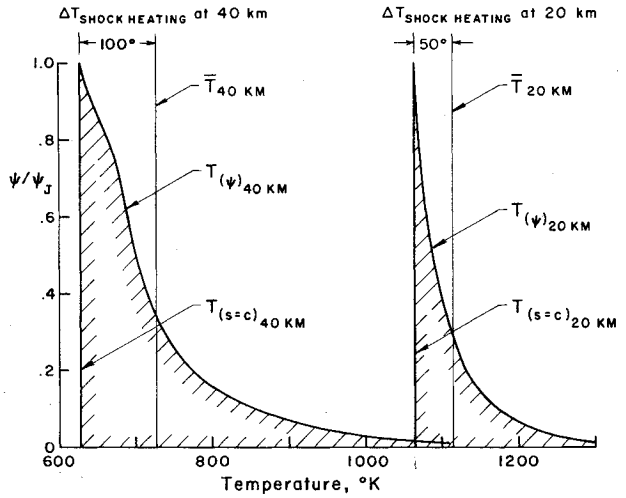

Fig. 10 Comparison of uniform and nonuniform pressure equilibrated startline temperatures as calculated by the SCIPPY code.

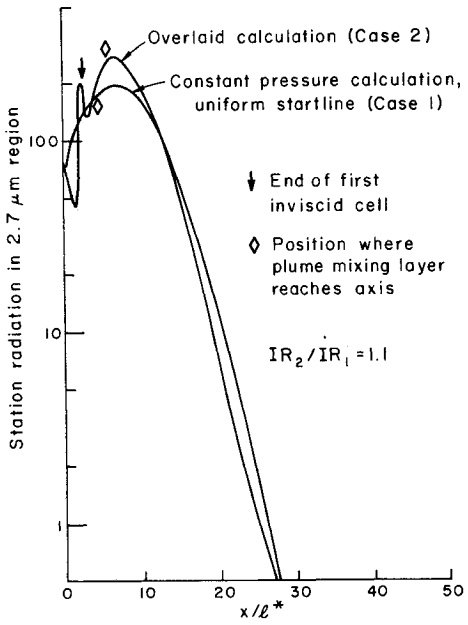

Fig. 11 Axial variation of station radiation for typical booster at lower altitude, overlaid vs. uniform startline.

chemical production rates on the local inviscid pressure and temperature variations can be significant in cases with fast combustion and is not treated in the pressure-equilibrated approach. The shock-dependent farfield nonuniformities also can affect plume emissions directly (i.e., plumes of homogeneous and nonhomogeneous central cores have different radiative characteristics) and indirectly through the influence on the farfield rates of mixing and afterburning.

Overlaid Approach

To account for the above effects in the simplest possible fashion, an overlaid approach employing the BOAT and SCIPPY codes was implemented. SCIPPY generated a detailed flowfield map of the inviscid/shock pattern in the first cell followed by a smooth decay to ambient pressure on an individual streamline basis. The map was read into the BOAT code which analyzed mixing and afterburning processes in the shear layer growing along the plume interface. The composite viscous/inviscid flow solution was supplied to the AARAD code for the ensuing radiative transfer calculations. This approach accounts for *all* the aforementioned contributions of inviscid/shock structure neglected in the pressure-equilibrated procedure. Certain simplifying assumptions have been made in the performance of these overlaid calculations (i.e., the neglect of the following: thermochemical processes in the inviscid solution, mixing in the Mach disk region, viscous/inviscid interactions, and external shock heating) which will somewhat influence the values of the predicted integrated signatures (see Ref. 1). These same assumptions are implicitly made in the pressure-equilibrated approach. The qualitative differences observed between results based on pressure-equilibrated and overlaid approaches should be unaffected by the use of such assumptions.

Table 1 Summary of rocket plume integrated signatures

Case	Lower (L) or higher (H) altitude	Inviscid structure	Turbulence parameters	Relative intensity[a]
1	L	Uniform startline	$k\epsilon 2$	0.42
2	L	Overlaid	$k\epsilon 2$	0.46
3	H	Uniform startline	$k\epsilon 2$	0.20
4	H	Overlaid	$k\epsilon 2$	0.61
5	H	Uniform startline (isentropic)	$k\epsilon 2$	0.09
6	H	Nonuniform startline	$k\epsilon 2$	0.34
7	L	Uniform startline	$k\epsilon 2$,cc	0.86
8	L	Overlaid	$k\epsilon 2$,cc	1.00
9	L	Uniform startline	D/G	0.61
10	L	Overlaid	$k\epsilon 2$, $Pr = 0.7$	0.29
11	H	Uniform startline	$k\epsilon 2$,cc	0.37
12	H	Overlaid	$k\epsilon 2$,cc	1.00
13	H	Overlaid	$k\epsilon 2$,cc, $Pr = 0.7$	0.76

[a] Intensities normalized by $k\epsilon 2$,cc overlaid predictions at lower and higher altitudes.

Comparisons of Signatures Calculated with Pressure-Equilibrated and Overlaid Modes of Operation

To assess the requirement for including the spatial details of the nearfield inviscid structure in the plume calculation, computations were performed for the aforementioned booster at representative lower and higher altitudes. At the lower altitude, shock strengths are moderate, afterburning is appreciable, and plume temperatures are high. At the higher altitude, shock strengths are substantial, afterburning is negligible, and plume temperatures are low.

At the lower altitude ($h < 20$-30 km), the spatial contributions of inviscid structure are expected to be rather small. This is confirmed by the comparison of the axial variation of station radiation (Fig. 11§) based on pressure-equilibrated (case 1) and overlaid (case 2) flowfield calculations. Here, the inviscidly induced excursions in radiation are small perturbations on the local station radiation. The integrated signatures (see Table 1) for cases 1 and 2 differ by only 10%.

At the higher altitude ($h > 30$-40 km), the spatial contributions of inviscid structure are found to be rather substantial as indicated by the corresponding comparison of radiation (Fig. 12) based on pressure-equilibrated (case 3) and overlaid (case 4) flowfield calculations. Here, the inviscidly induced excursions in radiation are pronounced and the overlaid approach yields integrated signature levels that are a factor of about 3 higher than those based on the pressure-equilibrated approach. It should be emphasized that both these flowfield calculations are based on inviscid solutions reflecting the same level of plume drag and, hence, the same total pressure losses. The signature differences are attributed to *how* these losses are incorporated into the flowfield

§The axial length in this and subsequent figures is scaled by a characteristic plume longitudinal length scale, l^*; $l^* = (F/q)^{1/2}$ where F is the thrust and q_∞ is the external flow dynamic pressure.

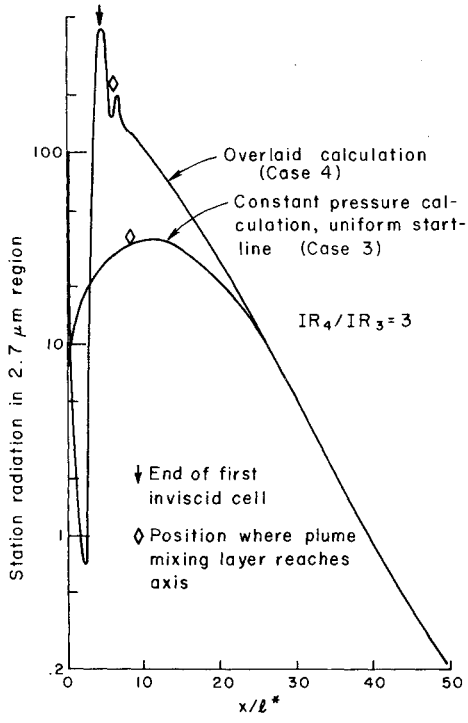

Fig. 12 Axial variation of station radiation for typical booster at higher altitude, overlaid vs uniform startline.

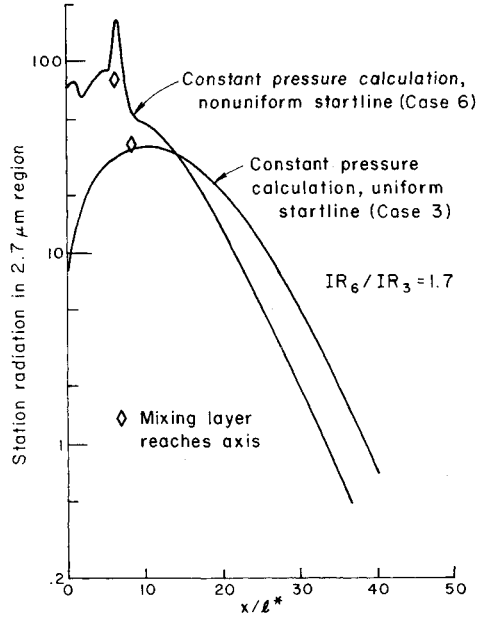

Fig. 13 Axial variation of station radiation for typical booster at higher altitude, uniform vs nonuniform startline.

solution. The effect on the integrated signature of the plume drag *only* can be ascertained by comparing pressure-equilibrated calculations made with isentropic (case 5) and "corrected" nonisentropic (case 3) uniform startlines. The signature level for the isentropic startline (case 5) is found to be lower than that for the nonisentropic startline (case 3) by a factor of 2. Hence, while the correct estimate of total pressure losses is quite significant at higher altitudes, the approach employed to incorporate these losses into the flowfield solution is of equal importance.

It had been conjectured[1] that the use of nonuniform startline conditions in a pressure-equilibrated mode of operation might prove adequate for signature-oriented studies. This approach treats the effects of nonlinear shock strengthening but neglects the nearfield wave structure. The comparisons (Fig. 13) between radiation for the uniform (case 3) and nonuniform (case 6) startline cases indicate that the spatial distributions are quite different, as are the integrated signature levels. However, while providing improvements over the uniform startline approach, the signature differences between the nonuniform and overlaid calculations indicate that the specific contributions associated with the nearfield wave structure are also quite substantial.

The conclusions drawn from these comparisons are:

1) At lower altitudes ($h<20$-30 km), the pressure-equilibrated approach with uniform startline conditions based on realistic plume drag estimates appears adequate for use in flight signature predictions for systems comparable to the one studied.

2) At higher altitudes ($h>30$-40 km), pressure-equilibrated approaches (with uniform or nonuniform startlines) are not adequate and the full spatial contributions of inviscid structure must be included in the flowfield representation.

3) For other systems, the altitude dependencies noted here may vary. Thus, for systems with larger chamber pressures and/or nozzle half angles, the spatial contributions of inviscid structure may be significant at even lower altitudes. Similar considerations apply for systems with different propellant and/or trajectory characteristics.

Signature Dependence on Turbulence Modeling Parameters

Rocket Plume Signature Dependence

Turbulent mixing is a dominant controlling mechanism in establishing the spatial variation of temperature and species concentration in a rocket exhaust. The rate of mixing controls the diffusion of species, the convection of thermal energy, and the conversion of kinetic energy into thermal energy through viscous dissipation. The characteristics of the afterburning processes also depend on the rate of mixing. While turbulence models are available that can accurately predict the mixing of low speed, nonreacting flows at constant pressure, their application to high speed, reacting flows with large pressure gradients (as encountered in rocket exhaust plumes) is uncertain. The manifestation of this uncertainty on plume fluid dynamical parameters has been presented in Refs. 7 and 8 largely through a comparison of results of several turbulence models with available laboratory data. The sensitivities imposed by this uncertainty on overall plume emission are addressed in this section.

In the previous section, the flowfield calculations were performed employing the kinetic energy/dissipation two-equation turbulence model[21] with a Prandtl number of unity. Previous applications of this $k\epsilon 2$ model to high speed mixing problems indicated that it overpredicted the rate of turbulent mixing.[1,7,8,21] To remedy this deficiency, a compressibility correction was introduced, ($k\epsilon 2$, cc model) whose assessment[22] indicated a marked improvement over the basic $k\epsilon 2$ model in application to those cases in the 1972 NASA Shear Flow Conference[23] which exhibited significant compressibility effects. Further comparisons with laboratory rocket plumes[1,8] showed that this compressibility correction was adequate in the plume nearfield, but in some situations tended to underpredict the farfield mixing rates. Since results using the basic and compressibility corrected $k\epsilon 2$ models generally tend to span the observed data (as illustrated for example, in the axial velocity decay results of Fig. 14 for a Mach 2.2 air jet exhausting into still air[24]), their use in this sensitibity study is appropriate. Also indicated in Fig. 14 are results obtained using the simple Donaldson/Gray (D/G)[25] eddy viscosity model. The predicted mixing rate is shown to be too fast in the initial region and too slow in the farfield.

For the lower altitude case discussed earlier, station radiation distributions, employing the basic $k\epsilon 2$ and com-

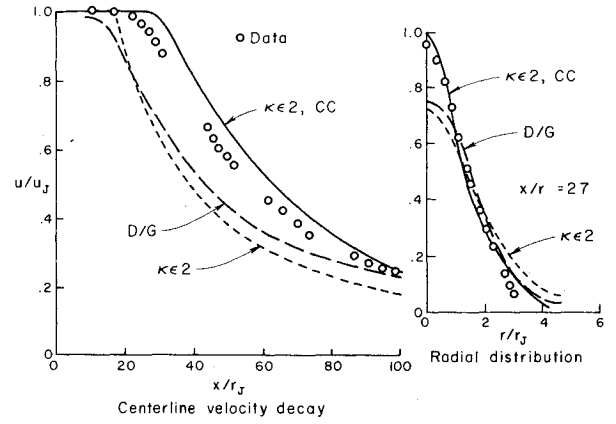

Fig. 14 Mach 2.2 air jet into still air, comparison of turbulence model predictions in BOAT with data (Eggers data from Ref. 24).

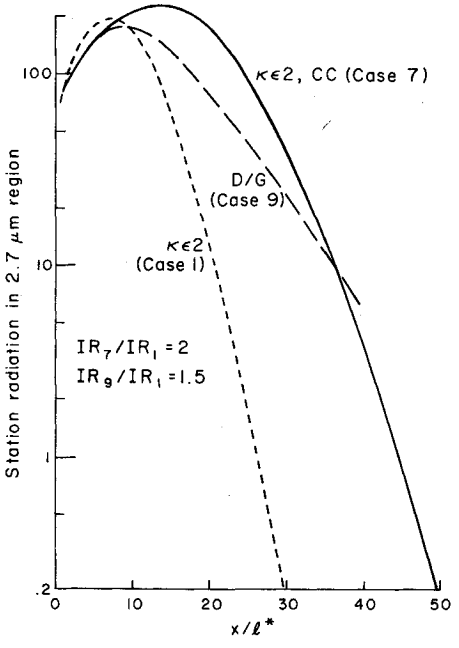

Fig. 15 Axial variation of station radiation for typical booster at lower altitude, uniform startline with several turbulence models.

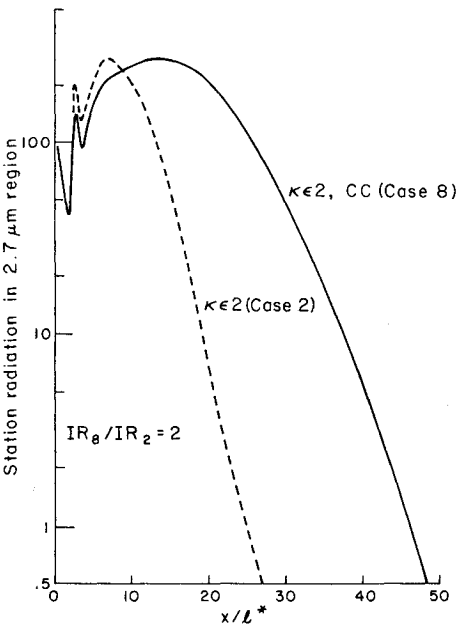

Fig. 16 Axial variation of station radiation for typical booster at lower altitude, overlaid results for two turbulence models.

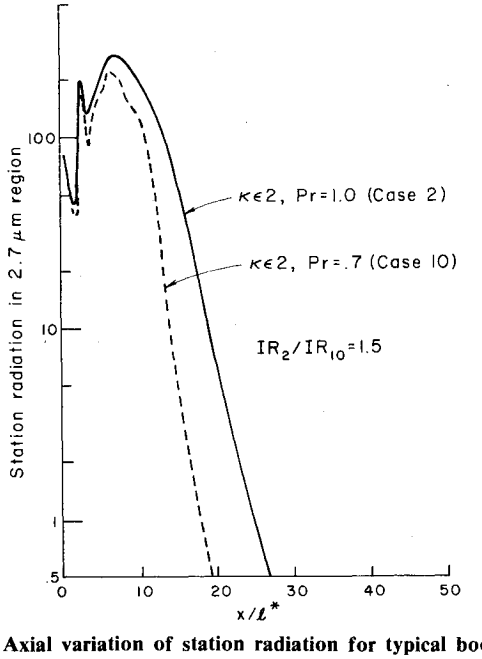

Fig. 17 Axial variation of station radiation for typical booster at lower altitude, effect of turbulent Prandtl number.

pressibility corrected $k\epsilon 2$, cc models, are markedly different for both the uniform startline (Fig. 15) and overlaid (Fig. 16) modes of operation. In terms of integrated signatures (see Table 1), the $k\epsilon 2$, cc results (case 7 for uniform startline and case 8 for overlaid) were higher than the basic $k\epsilon 2$ results (cases 1 and 2) by factors of about 2 in both modes of operation. The negligible contribution of inviscid structure at lower altitudes, using both turbulence models, is quite evident.

Since there has been rather extensive usage of the LAPP code[2] in conjunction with the D/G eddy viscosity model[25] in past signature studies, it is of interest to see how this turbulence model fares in this situation. Incorporation of this model in the BOAT code with uniform startline conditions should yield results comparable to those of LAPP. The resultant axial distribution of station radiation is shown in Fig. 15. The peak intensity occurs at an axial location between that of the two $k\epsilon 2$ models and its magnitude is somewhat lower than predicted by either of them. The farfield decay rate, however, is markedly less than that predicted by either of the two $k\epsilon 2$ models. In terms of the integrated signature level, the D/G model results (case 9) are about 40% less than the $k\epsilon 2$, cc model results. Comparisons of D/G model predictions with laboratory data (see Refs. 7 and 8) have demonstrated that, in general, its overall performance is rather poor. In this situation, 90% of the total radiation in the D/G calculation comes from the region where $x/l^* < 25$ which corresponds to about 100 jet radii. By analogy with its performance in predicting the Eggers data (Fig. 14), the mixing is initially much too fast and, then, substantially too slow. Thus, by locally incorrect rates of mixing, a somewhat reasonable integrated signature level is achieved.

In all calculations thus far, the turbulent Prandtl number was set to unity. In most past analytical studies of rocket plume flowfields, the Prandtl number has been varied between 0.7 and 1. To assess the effect of this type of variation on the plume signature level, the overlaid $k\epsilon 2$ calculation was repeated with a Prandtl number of 0.7 (case 10). The resultant axial distribution of station radiation is shown in Fig. 17. The

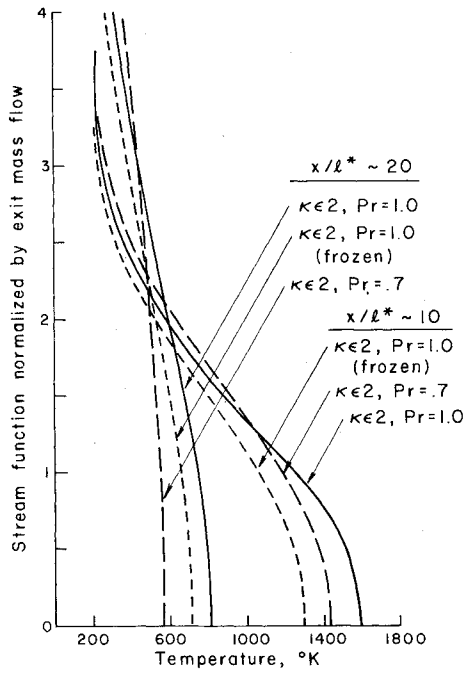

Fig. 18 Temperature profiles at $X/l^* = 10$ and 20 for typical booster at lower altitude.

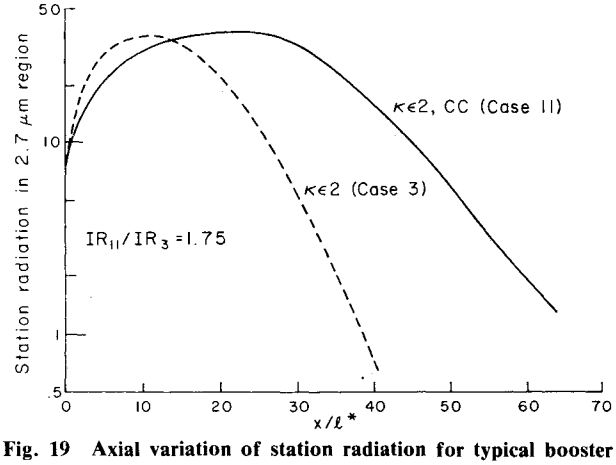

Fig. 19 Axial variation of station radiation for typical booster at higher altitude, uniform startline results for two turbulence models.

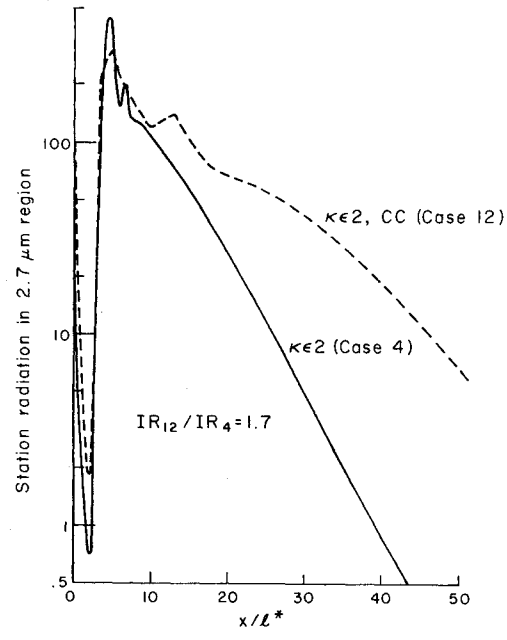

Fig. 20 Axial variation of station radiation for typical booster at higher altitude, overlaid results for two turbulence models.

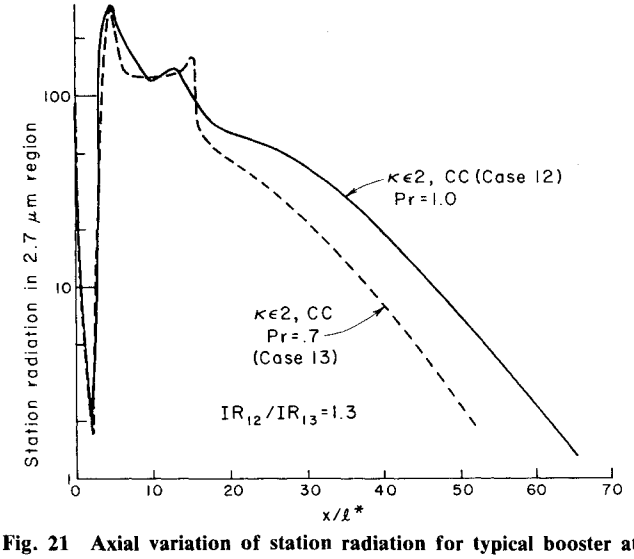

Fig. 21 Axial variation of station radiation for typical booster at higher altitude, effect of turbulent Prandtl number.

change due to decreasing the Prandtl number is quite marked and yields a reduction in integrated signature of about 60%. The temperature profiles at $x/l^* = 10$ and 20 for $Pr = 1$ and 0.7 are shown in Fig. 18. It is noteworthy that the signature reduction associated with the total neglect of chemistry (the frozen profiles are also depicted in Fig. 18) in this case is comparable to that associated with reducing the Prandtl number from 1 to 0.7. Thus, for this chemical system, "fine tuning" the chemical reaction mechanism and associated rate coefficients will not yield appreciably better signature predictions. A more fundamental and important issue is the determination of appropriate values of the turbulent Prandtl number, as a function of relevant plume parameters.

At higher altitudes, the sensitivity to variations in the turbulence models is comparable to that in the lower altitude cases as exhibited in the station radiation distributions for the uniform startline (Fig. 19) and overlaid (Fig. 20) calculations. Here, regardless of the turbulence model employed, the effects of inviscid structure are quite appreciable. For the uniform startline cases, the integrated signature based on using the $k\epsilon 2$, cc model (case 11) was about 80% higher than that using the basic $k\epsilon 2$ model (case 3). In the overlaid cases, the $k\epsilon 2$, cc model results (case 12) were about 65% higher (than case 4). Hence, the significant contribution of nearfield inviscid processes tends to somewhat desensitize the effects of turbulence model variations. The sensitivity to varying the turbulence Prandtl number is depicted in Fig. 21 for overlaid calculation using the $k\epsilon 2$, cc model. The integrated signature with $Pr = 0.7$ (case 13) is reduced by 45% (over that of case 12).

The integrated signature results for all the cases discussed are summarized in Table 1. The results are nondimensionalized by the integrated signatures obtained for the overlaid $k\epsilon 2$, cc calculations with $Pr = 1$ at both the lower and higher altitudes studied.

With the sensitivities to both turbulence modeling parameters and inviscid operational modes exhibited, an obvious question arises: How do the predictions compare with the observed flight data? This issue is not explored here since comparisons of predicted and observed integrated signatures *cannot* isolate modeling deficiencies. There are several additional assumptions employed in these calculations which

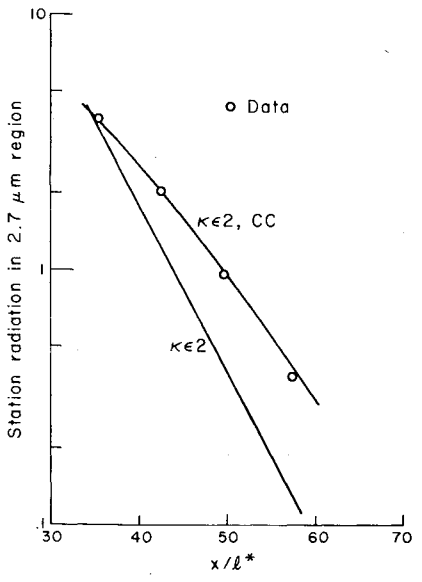

Fig. 22 Comparison of predicted farfield decay in station radiation with observations for typical booster at higher altitude.

will affect the overall signature level and for which sensitivities have not as yet been explored. However, the availability of spatially resolved radiation data can shed some light on the adequacy of farfield predictions. Farfield decay *rates* are not dependent upon nearfield approximations and can be used to validate predicted rates of turbulent mixing. In Fig. 22, the predicted farfield decay of station radiation at the higher altitude is compared with observed data. The curves have been shifted only vertically to coincide levels at the start (so that rate differences may be readily distinguished). The agreement with the $k\epsilon 2$, cc model is quite good, while the basic $k\epsilon 2$ model is predicting a much faster rate of farfield mixing.

Conclusions

The specific influence of inviscid/shock processes on rocket plume emissions has been exhibited via incorporation of these processes into a flowfield model in varying levels of physical realism. At the lowest level, the "global" contribution of shock losses is incorporated yielding pressure-equilibrated startline conditions for a farfield mixing analysis. This approach appears to be adequate for lower altitude ($h < 20$-30 km) flight signature studies for systems comparable to the one studied here. For systems with different propellants and/or vehicle/engine trajectory characteristics, the adequacy of this simplified procedure requires further assessment.

At higher altitudes ($h > 30$-40 km), the global inclusion of shock losses does *not* provide an adequate representation of the flowfield structure. In the nearfield, pressure and temperature variations associated with the inviscid wave structure influence signature levels both directly and indirectly through their effect on mixing and thermochemical processes. In addition, both shock and mixing processes in the nearfield influence the starting profiles of mean flow and turbulence variables for the farfield analysis.

A simplified overlaid procedure has been introduced which accounts for the above contributions of inviscid/shock processes. This overlaid procedure introduces a substantially more realistic flowfield representation than the pressure-equilibrated approach. Many of the simplifying assumptions employed here, in the preliminary use of this procedure, can be readily eliminated and the overlaid approach appears to be quite promising for flight signature studies.

For the analysis of laboratory infrared data, where the spatially resolved signatures display the contributions of inviscid structure for several cell lengths, an overlaid procedure is not generally adequate and a fully coupled approach is required. The requirement for using a fully coupled approach in flight signature studies has not heretofore been demonstrated. While situations arise where nearfield interactive effects will influence the local flow structure, the specific contribution of such interactions on overall plume emission must be quantified.

The sensitivity of turbulence model parameters has been demonstrated via the use of several turbulence models and turbulent Prandtl numbers of 0.7 and 1 in performing the flowfield calculations. The effect of these variations on plume emission was shown to be important. This highlights the need for establishing turbulence modeling parameters which can be used for predicting high-speed reacting flows with some degree of reliability and universality.

This assessment study has served to highlight the dependence of predicted plume infrared radiation on selected gasdynamic modeling assumptions and parameters for a particular system. Clearly, analogous studies are required for other types of systems (viz., systems with exotic and/or high-energy propellants, solid propellants, etc.) and an expanded choice of parameters must be investigated. The following parameters are of particular importance:

1) For particle laden plumes, one requires sensitivities to uncertainties in the particle drag/heat transfer laws and size distribution as well as to gas/particle equilibration assumptions (see Ref. 12).

2) For exotic propellant systems, large uncertainties exist in the chemical rates and radiative band model parameters whose impact on signature levels requires determination.

3) The inclusion of turbulence/chemistry interactions in the flowfield calculation and turbulence/radiative interactions in the radiative transfer calculations can influence signature levels. The signature dependence on such interactions requires determination.

4) The inclusion of viscous/inviscid interactions along the plume interface (particularly when large base and/or separated regions exist) and the Mach disk slipstream can appreciably alter the plume flow pattern. The impact of such interactions on plume signature levels requires consideration.

Such assessment studies are now in progress and salient findings will be reported in subsequent publications.

Acknowledgments

This work was supported by the JANNAF Exhaust Plume Technology Committee (monitored by Army Missile R&D Command) under Contract. DAAK40-78-C-0124 and by the Naval Weapons Center Optical Signatures Program under Contract. N00123-78-C-0010.

References

[1] Dash, S.M. and Pergament, H.S., "The Analysis of Low Altitude Rocket and Aircraft Plume Flowfields: Modeling Requirements and Procedures," *Proceedings of the JANNAF 10th Plume Technology Meeting*, CPIA Pub. 291, Vol. I, 1977, pp. 53-132.

[2] Mikatarian, R.R., Kau, C.J., and Pergament, H.S., "A Fast Computer Program for Nonequilibrium Rocket Plume Predictions," AFRPL-TR-72-94, Aug., 1972.

[3] Dash, S.M., Pergament, H.S., and Thorpe, R.D., "A Modular Approach for the Coupling of Viscous and Inviscid Processes in Rocket Exhaust Plumes," AIAA Paper 79-0150, New Orleans, La., Jan., 1979.

[4] Dash, S.M., Pergament, H.S., and Thorpe, R.D., "The JANNAF Standard Plume Flowfield Model: Modular Approach, Computational Features and Preliminary Results," *Proceedings of the JANNAF 11th Plume Technology Meeting*, CPIA Pub. 306, Vol. I, 1979, pp. 345-442.

[5] Dash, S.M. and Pergament, H.S., "A Computational Model for the Prediction of Jet Entrainment in the Vicinity of Nozzle Boattails (The BOAT Code)," NASA CR-3075, Dec., 1978.

[6] Dash, S.M., Wilmoth, R.G., and Pergament, H.S., "Overlaid Viscous/Inviscid Model for the Prediction of Nearfield Jet Entrainment," *AIAA Journal*, Vol. 17, Sept. 1979, pp. 950-58.

[7] Pergament, H.S., Dash, S.M., and Fishburne, E.S., "Methodology for the Evaluation of Turbulence Models for Afterburning Rocket and Aircraft Plumes," *Proceedings of the JANNAF 10th Plume Technology Meeting*, CPIA Pub. 291, Vol. I, 1977, pp. 133-72.

[8] Pergament, H.S., Dash, S.M., and Varma, A.K., "Evaluation of Turbulence Models for Rocket and Aircraft Plume Flowfield Predictions," AIAA Paper 79-0359, New Orleans, La., Jan., 1979.

[9] Dash, S., Boccio, J., and Weilerstein, G., "A Computational System for the Prediction of Low Altitude Rocket Plume Flowfields: Volume I-Integrated System, Volume II-Inviscid Plume Model (MAXIPLUM), Volume III-Mixing/Afterburning Model (CHEMX)," General Applied Science Laboratories, Inc., Westbury, N.Y.., TR-239, Dec. 1976.

[10] Wilmoth, R.G., Dash, S.M., and Pergament, H.S., "A Numerical Study of Jet Entrainment Effects on the Subsonic Flow Over Nozzle Afterbodies," AIAA Paper 79-0135, New Orleans, La., Jan. 1979.

[11] Dash, S.M. and Thorpe, R.D., "A New Shock-Capturing/Shock-Fitting Computational Model for Analyzing Supersonic Inviscid Flows (The SCIPPY Code)," Aeronautical Research Associates of Princeton, Inc., Report 366, Nov., 1978.

[12] Thorpe, R.D., Dash, S.M., and Pergament, H.S., "Inclusion of Gas/Particle Interactions in a Shock Capturing Model for Nozzle and Exhaust Plume Flows," AIAA Paper 79-1288, Las Vegas, Nev., June 1979.

[13] Dash, S.M., "Preliminary Calculations of Supersonic Viscous/Inviscid Interactions Using the Fully-Coupled Version of the SCIPPY Code," Aeronautical Research Associates of Princeton, Inc., Tech. Memo. 79-3, Feb. 1979.

[14] Pergament, H.S., Fishburne, E.S., Abuchowski, S., Pearce, B.E., and Dash, S.M., "The Naval Weapons Center Target Signature Code," Aeronautical Research Associates of Princeton, Inc., Report 380, Feb., 1979.

[15] Ludwig, C.B., Malkmus, W., Reardon, J.E., and Thomson, J.A.L., *Handbook of Infrared Radiation from Combustion Gases*, NASA SP-3080, 1973.

[16] Young, S.J., "Band Model Parameters for the 2.7μm Bands of H_2O and CO_2 in the 100 to 3000 K Temperature Range," Space and Missile Systems Organization, TR-75-209, July 1973.

[17] Sukanek, P.C., "Matched Pressure Properties of Low Altitude Plumes," *AIAA Journal*, Vol. 15, Dec. 1977, pp. 1818-21.

[18] Pearce, B.E. and Dash, S.M., "Use of Matched Pressure Initial Conditions for Predicting Low Altitude Rocket Plume Radiation," *AIAA Journal*, Vol. 17, June 1979, pp. 667-70.

[19] Wilson, K.H., personal communication, Lockheed Palo Alto Research Laboratory, Nov., 1978.

[20] Marvin, J.G., "Turbulence Modeling for Compressible Flows," NASA TM X-73, 188, Jan., 1977.

[21] Launder, B.E., Morse, A., Rodi, W., and Spalding, D.B., "Prediction of Free Shear Flows: A Comparison of Six Turbulence Models," *Free Turbulent Shear Flows*, Vol. I, NASA SP-321, July 1972, pp. 361-426.

[22] Dash, S.M., Weilerstein, G., and Vaglio-Laurin, R., "Compressibility Effects in Free Turbulent Shear Flows," Air Force Office of Scientific Research, TR-75-1436, Aug., 1975.

[23] Anon., *Free Turbulent Shear Flows*, Vols. I and II, NASA SP-321, July 1972.

[24] Eggers, J.M., "Velocity Profiles and Eddy Viscosity Distributions Downstream of a Mach 2.22 Nozzle Exhausting to Quiescent Air," NASA TN D-3601, 1966.

[25] Donaldson, C. duP. and Gray, K.E., "Theoretical and Experimental Investigation of the Compressible Free Mixing of Two Dissimilar Gases," *AIAA Journal*, Vol. 4, 1966, pp. 2017-25.